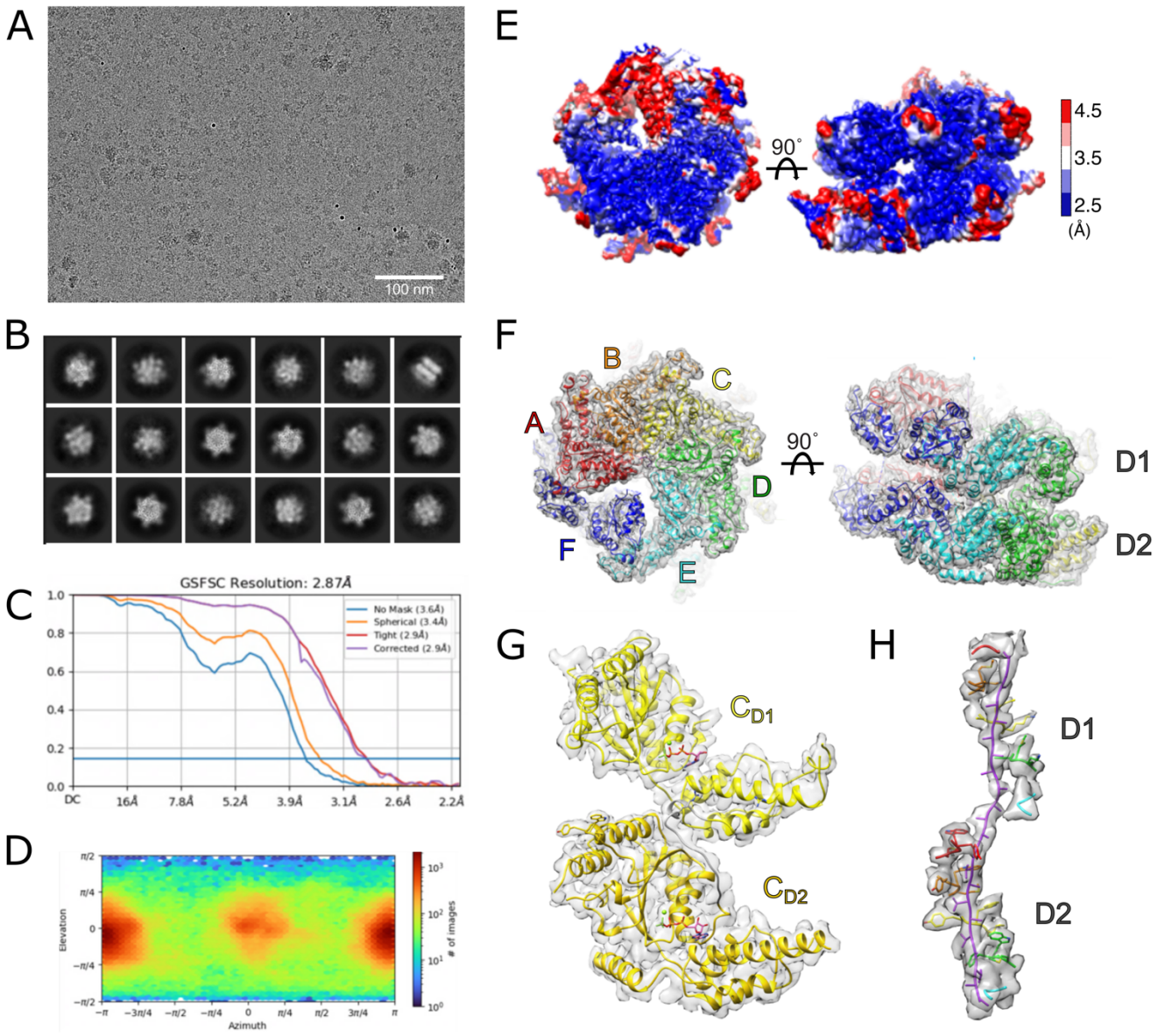

Supplementary Figure 1. Consensus structure of Cdc48 bound to substrate. (A) Cryo-EM micrograph of native Cdc48-Shp1 complexes. (B) CryoEM 2D class averages of selected particles. (C) Gold standard FSC plot of 2.9 Å consensus reconstruction. (D) Orientation distribution plot. (E) Local resolution heat map. (F) Consensus map density is zoned around displayed residues within 2.5 Å at 3.5-σ threshold. (G) Model and density at 6.5-σ threshold of subunit C. (H) Density of pore loop interactions with the substrate displayed at 4-σ threshold.

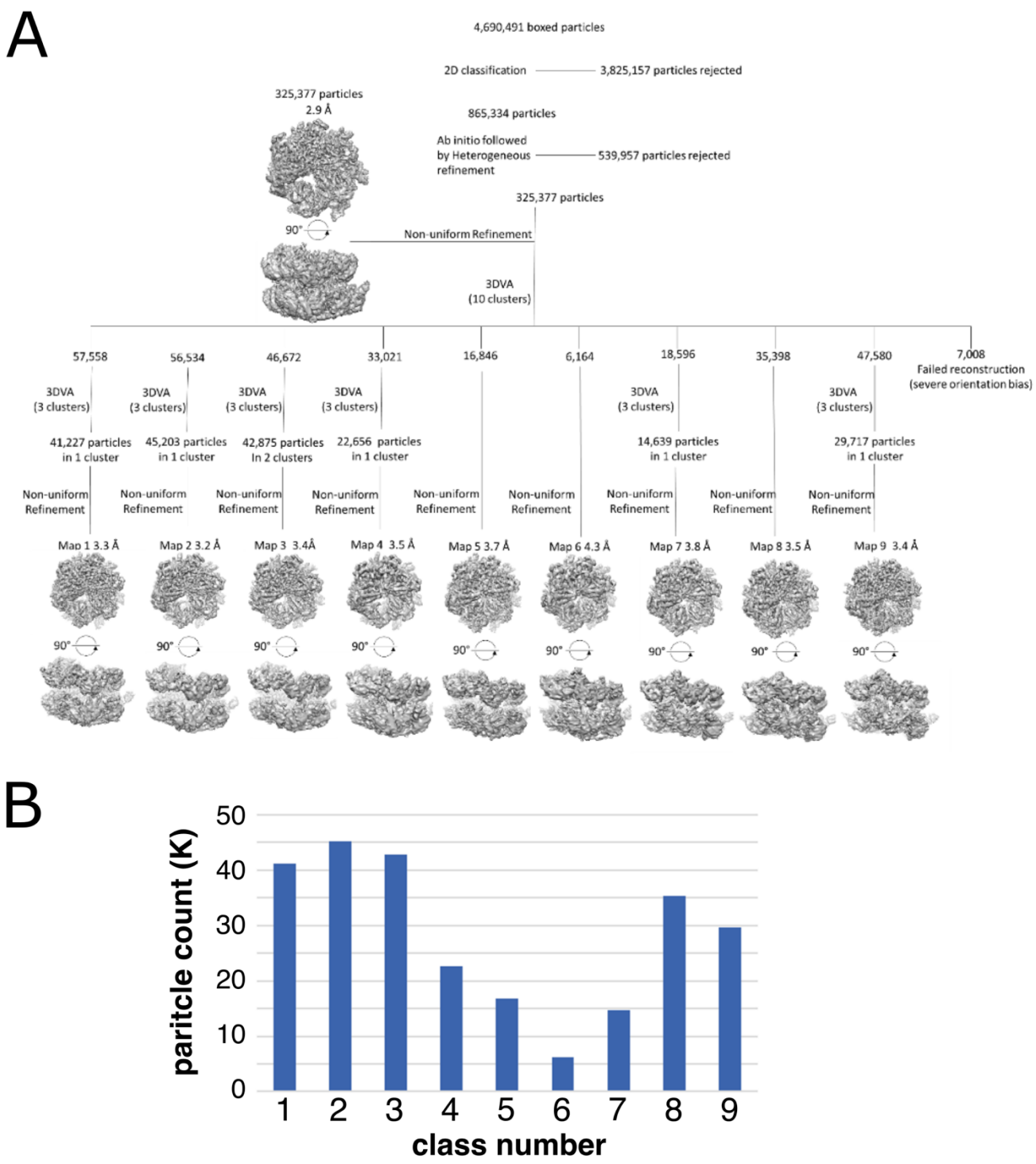

Supplementary Figure 2. Cryo-EM image processing. (A) Image processing workflow. (B) Particle number distribution.

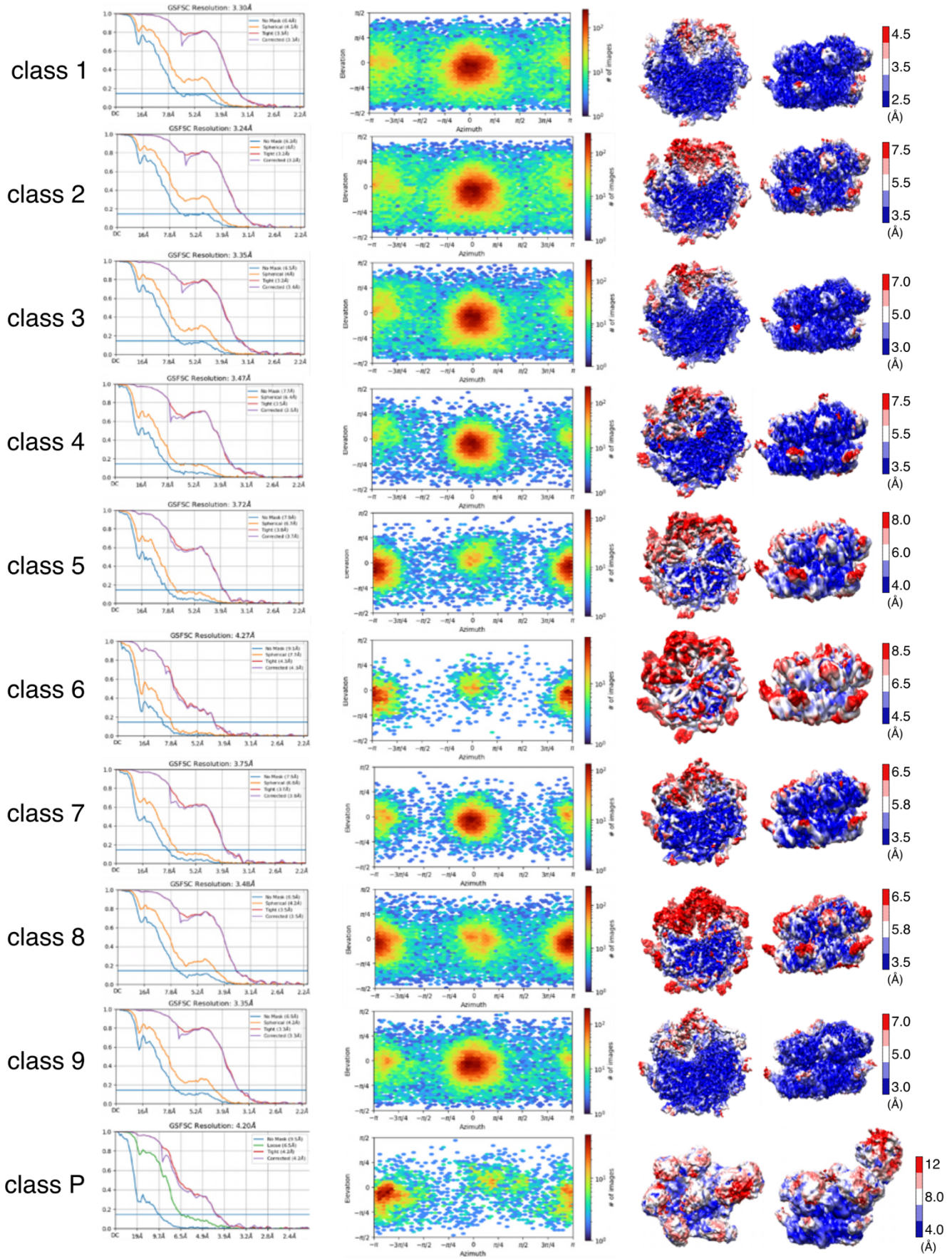

Supplementary Figure 3. Cryo-EM reconstruction validation. Gold standard FSC (left), orientation distribution plot (middle), and local resolution heat map (right).

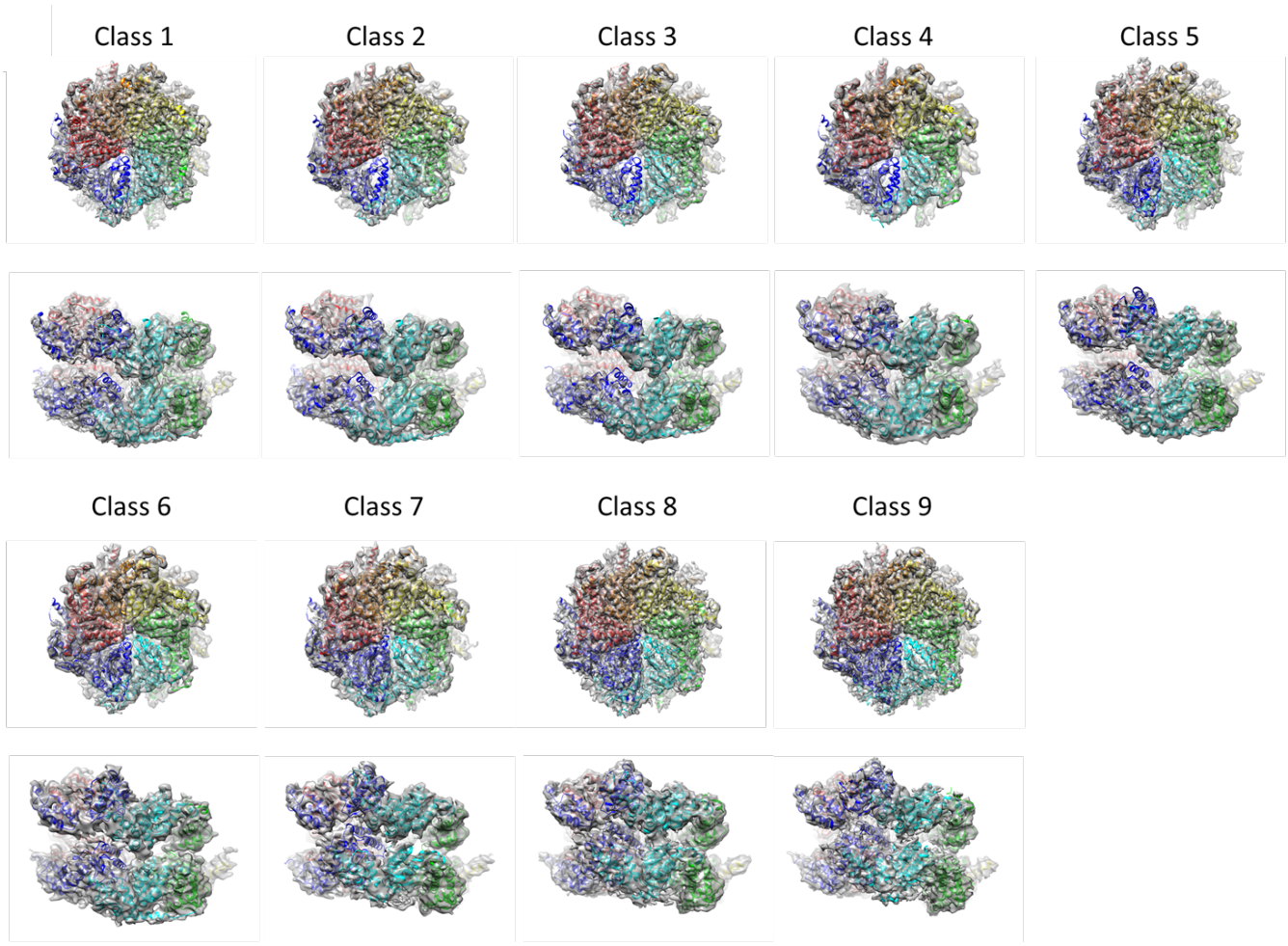

Supplementary Figure 4. 3D Variability Analysis reveals 9 distinct classes with variable positioning of mobile subunits D, E, and F. Fits of class 1-9 models into their respective maps at 4σ threshold level.

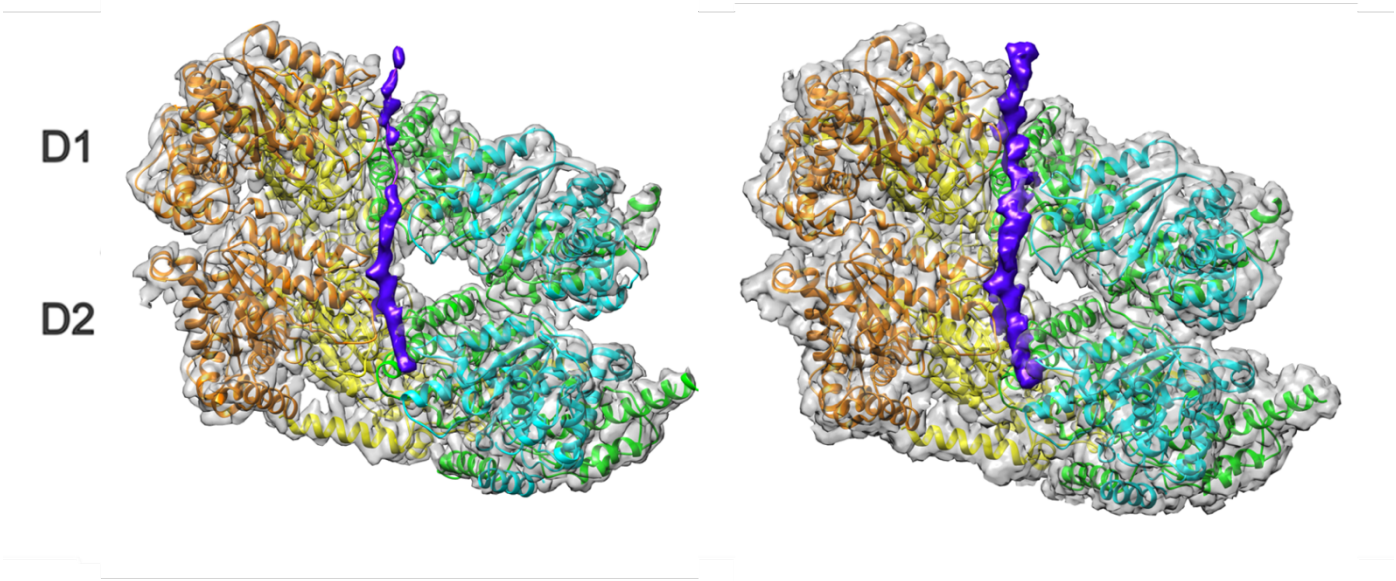

Supplementary Figure 5. Substrate density at high and low thresholds. Substrate density in purple with density displayed at 6σ (left) and at 2.5σ (right).

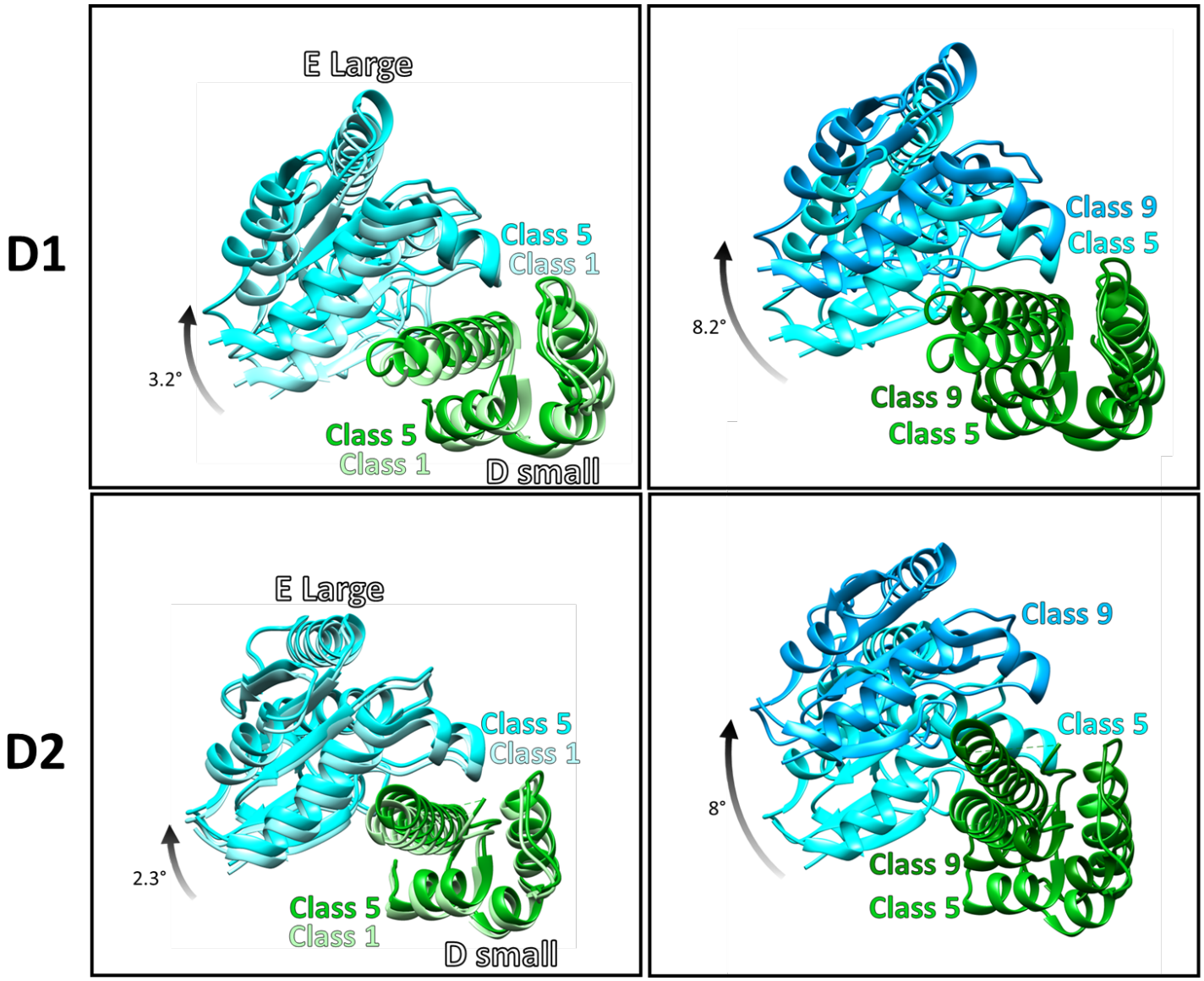

Supplementary Figure 6. Simultaneous movement of adjacent large and small subunits. Classes aligned by the overlap of subunits B and C. Class 1, 5, and 9 subunit D small domain displayed in lime green, green, and dark green, respectively. Class 1, 5, and 9 Large domain of subunit E displayed in light blue, cyan, and dodger blue. Positions are displayed for D1(top) and D2(bottom).

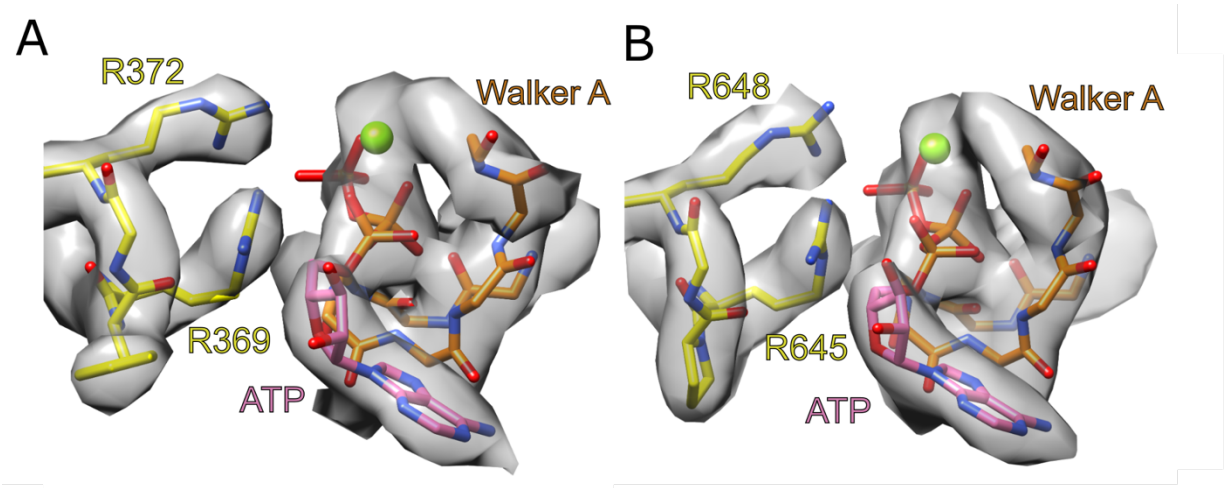

Supplementary Figure 7. Coordination between arginine fingers and ATP. (A) D1 nucleotide binding pocket at the subunit BC interface with Walker A from subunit B (orange) and arginine fingers (R369, R372) from subunit C (yellow). Threshold at 7.5σ. (B) D2 nucleotide binding pocket with residues as in A. Threshold at 8.75σ. Green sphere denotes Mg^{2+}; nucleoside shown in pink; phosphates and BeF_x denoted in orange.

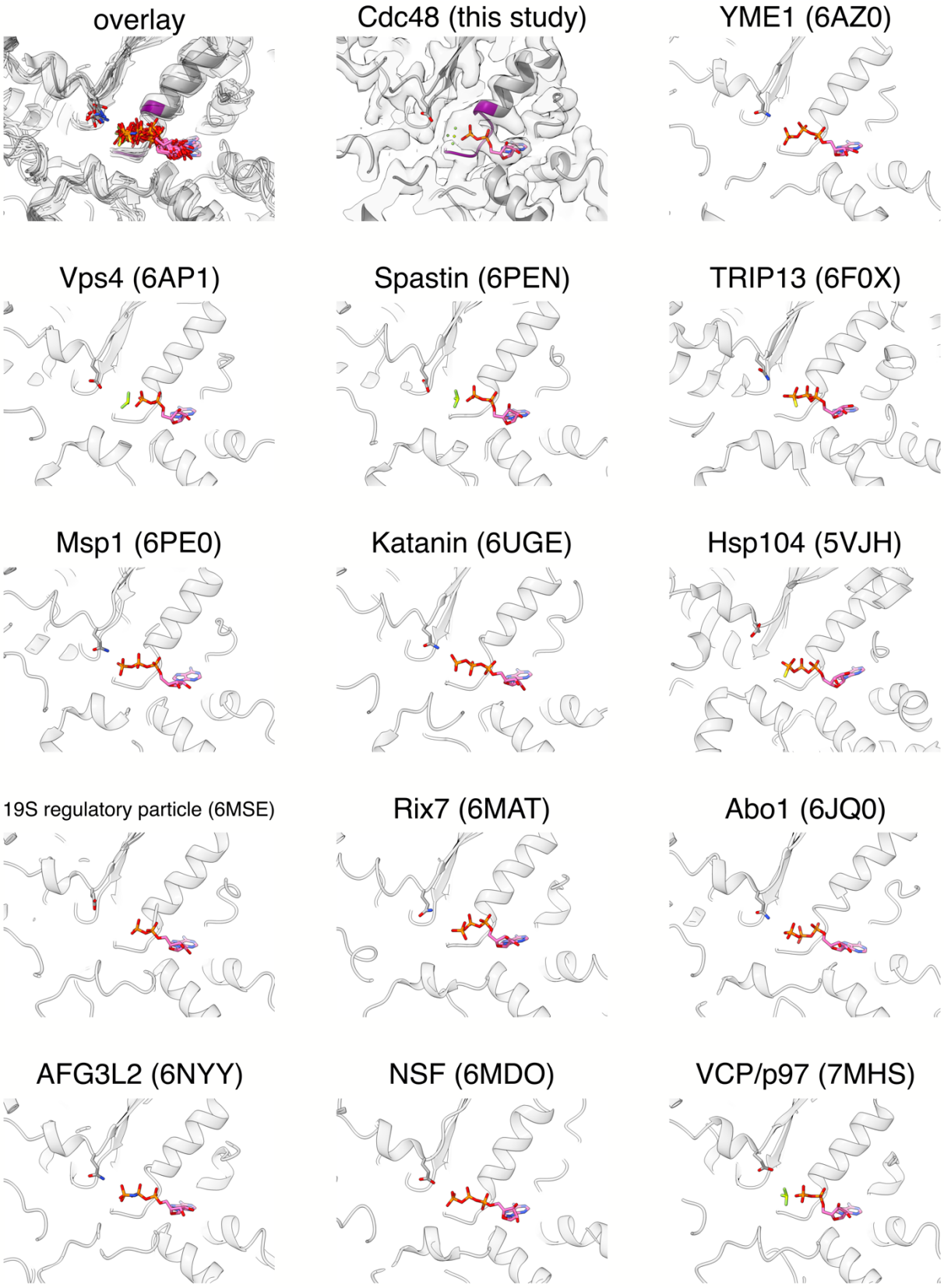

Supplementary Figure 8. Structures of AAA+ ATPase ATP-binding pockets. The top left panel is an overlay of 14 structures of ATP or ATP-like bound AAA+ ATPases. Individual structures and their corresponding PDB accession numbers are shown in other panels. Nucleotide and Walker B residues shown as sticks. Walker A motif shown as purple ribbon in the Cdc48 panel as a reference.

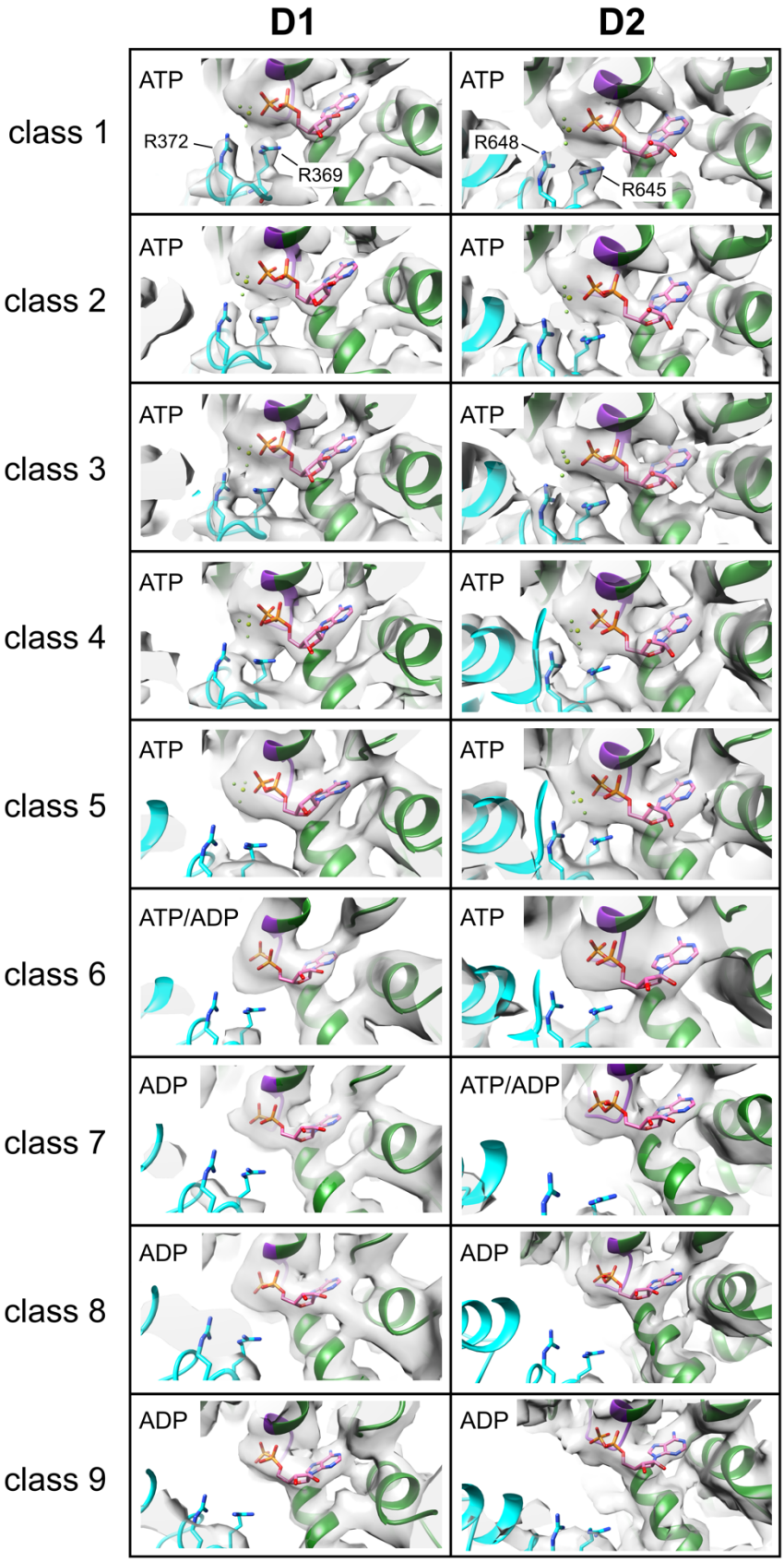

Supplementary Figure 9. Model and density of the subunit D nucleotide binding pocket (DE interface). Walker A, purple ribbon (D1, residues 255-262; D2, residues 528-535). Arginine finger residues in subunit E shown as cyan sticks (D1, residues R369, R372; D2, residues R645, R648). ADP displayed as pink sticks and BeF_x as green spheres.

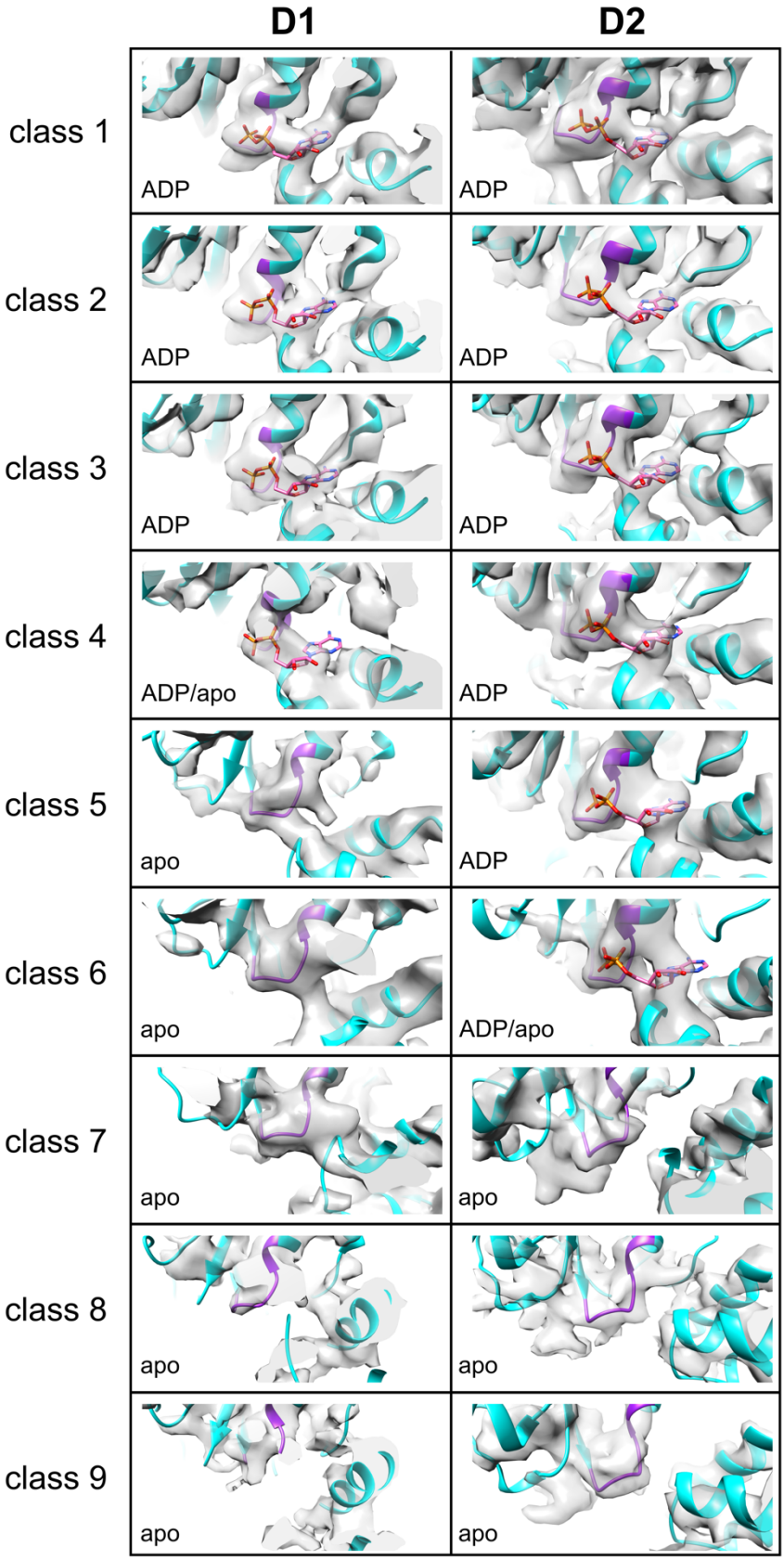

Supplementary Figure 10. Model and density of the subunit E nucleotide binding pocket (EF interface). Walker A, purple ribbon (D1, residues 255-262; D2, residues 528-535). ADP displayed as pink sticks.

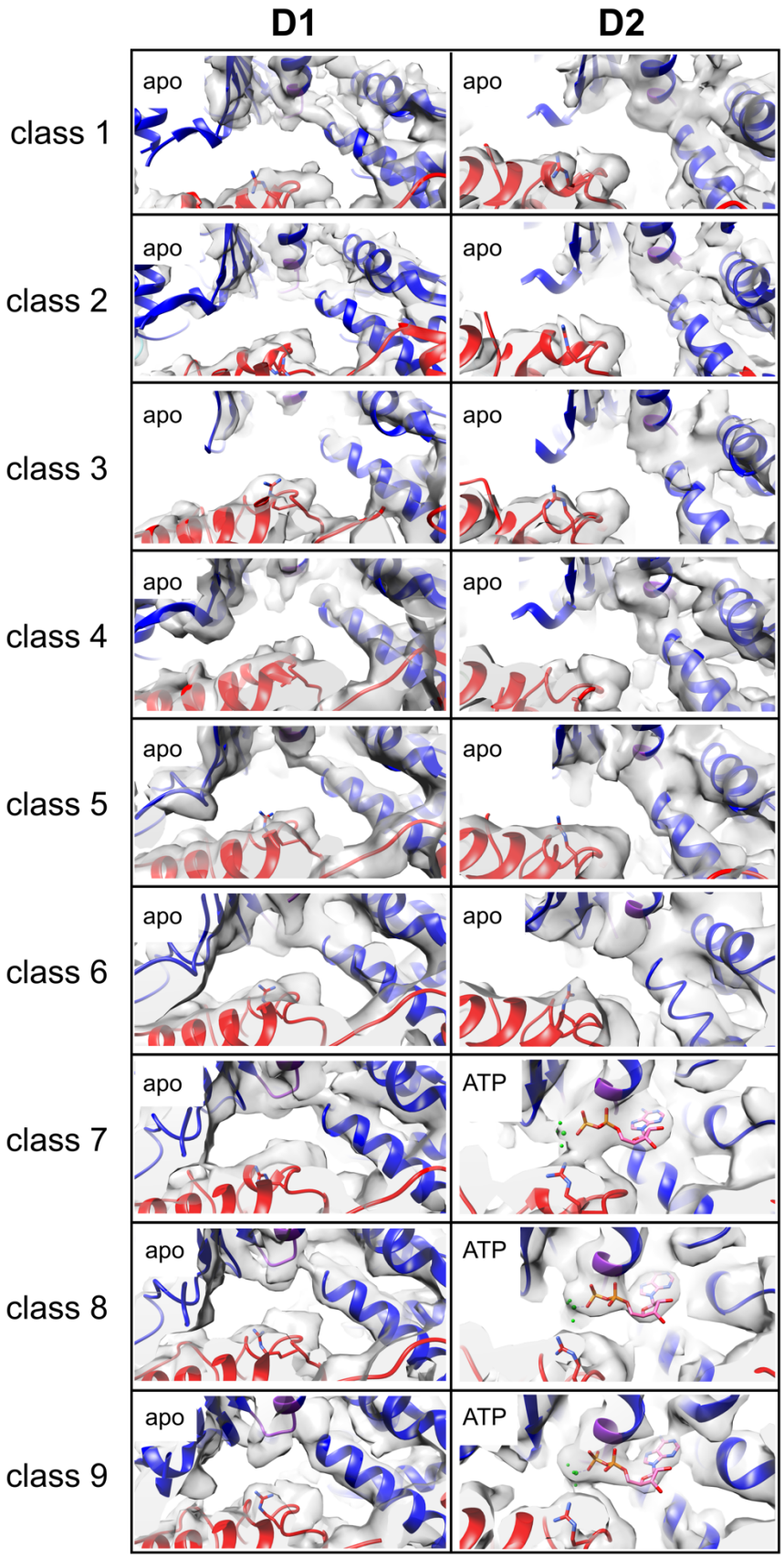

Supplementary Figure 11. Model and density of the subunit F nucleotide binding pocket (FA interface). Walker A, purple ribbon (D1, residues 255-262; D2, residues 528-535). Arginine finger residues in subunit A shown as red sticks (D1, residues R369, R372; D2, residues R645, R648). ADP displayed as pink sticks and BeF_x as green spheres.

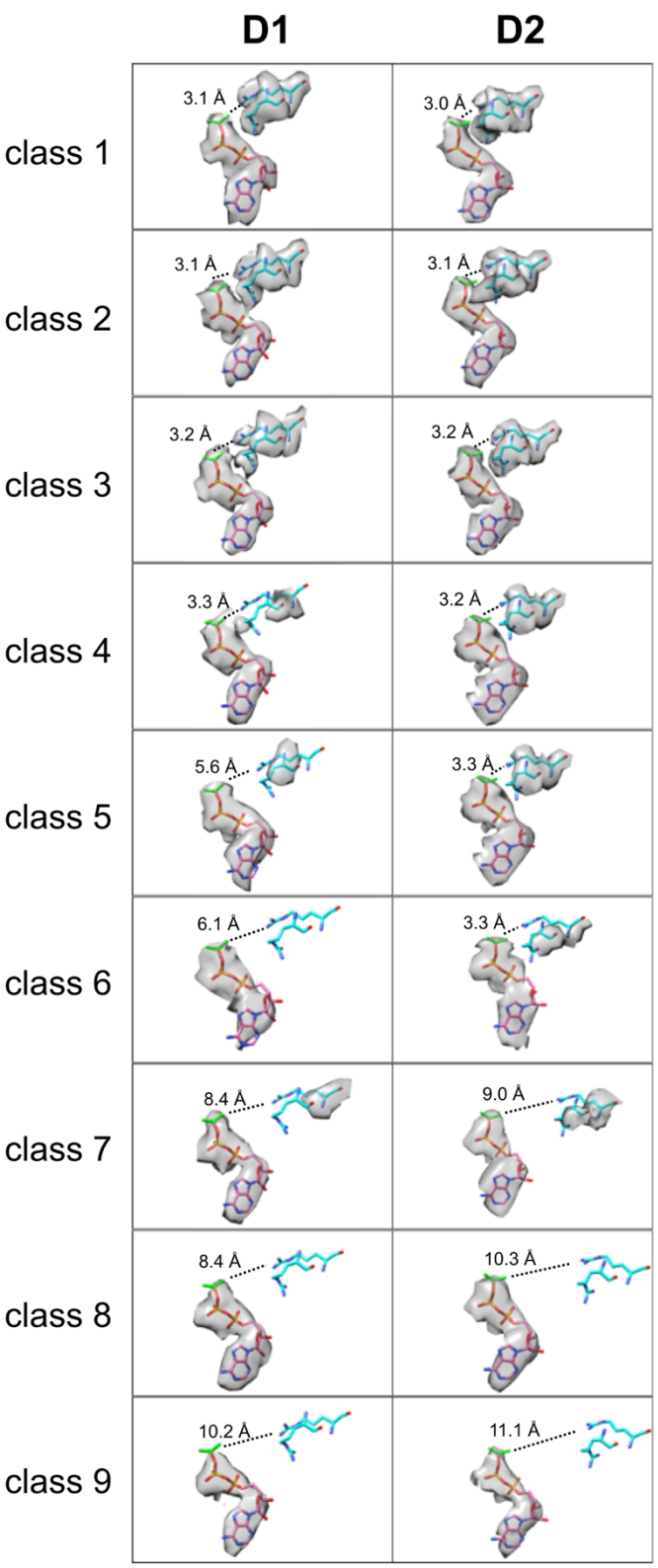

Supplementary Figure 12. Displacement of arginine fingers at the DE interface during subunit movement. Model and density of ATP and arginine finger positions at the DE interface. ADP•BeF_x fit into all classes from the consensus structure by alignment of the Walker A domain. Arginine finger positions are predicted based on the fitting of the large ATPase domain of E as a rigid body. D1 (left) and D2 (right). Density displayed at 6.5 σ. Arginine fingers in cyan, nucleotide in pink. Distances measured from NH2 of R372 and R648 in D1 and D2 respectively relative to F3 of BeF_x (dashed lines). The density for BeF_x weakens as arginine fingers separate from nucleotide.

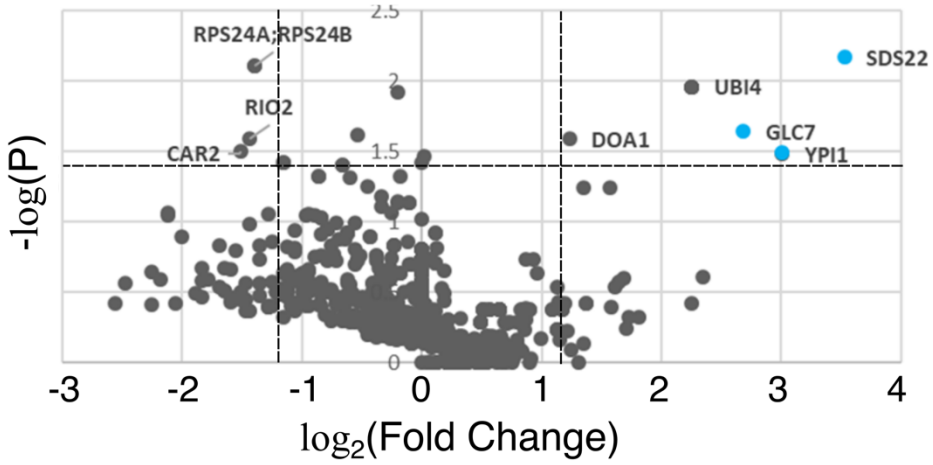

Protein	Fold Change (log_2)	P value -log(P)	Peptide sequences	Coverage percentage
Sds22p	3.5	2.2	28	82%
Ypi1p	3.0	1.5	12	52%
Glc7p	2.7	1.6	17	52%
Ubi4p	2.3	2.0	15	90%
Doa1p	1.2	1.6	57	77%
Dbp2p	-1.2	1.4	22	50%
Rps24A	-1.4	2.1	4	29%
Rio2p	-1.4	1.6	6	19%
Car2p	-1.5	1.5	73	80%

Supplementary Figure 13. Mass spectrometry proteomics of ATP elutions from Shp1 co-IPs. Top, Volcano plot of detected proteins from Shp1-FLAG co-IPs eluted with ATP over ADP•BeF_x controls. Bottom, list of proteins with $-\log(P) \geq 1.4$ and $\log_2$(fold change) $\geq |1.2|$. n=3 for each sample.

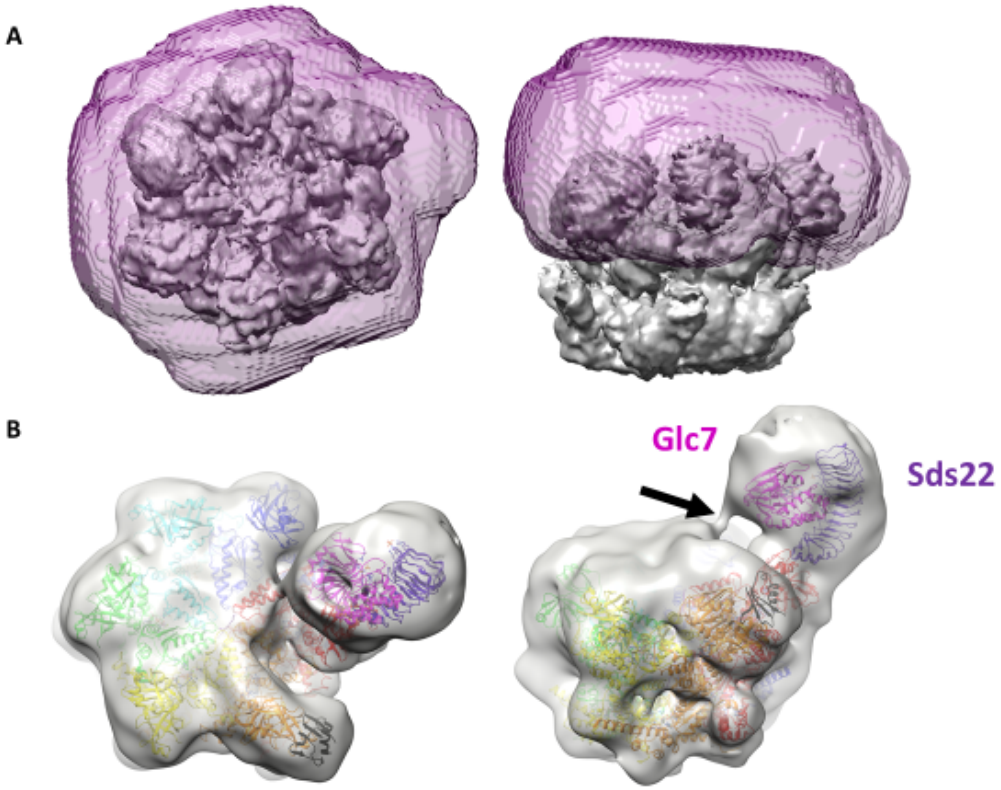

Supplementary Figure 14. Image processing of PP1-containing class (class P). (A) Mask used for 3DVA of Cdc48 N-terminal domains. (B) Map at 1σ reveals connecting density between Glc7-Sds22 to the Cdc48 central pore (arrow).

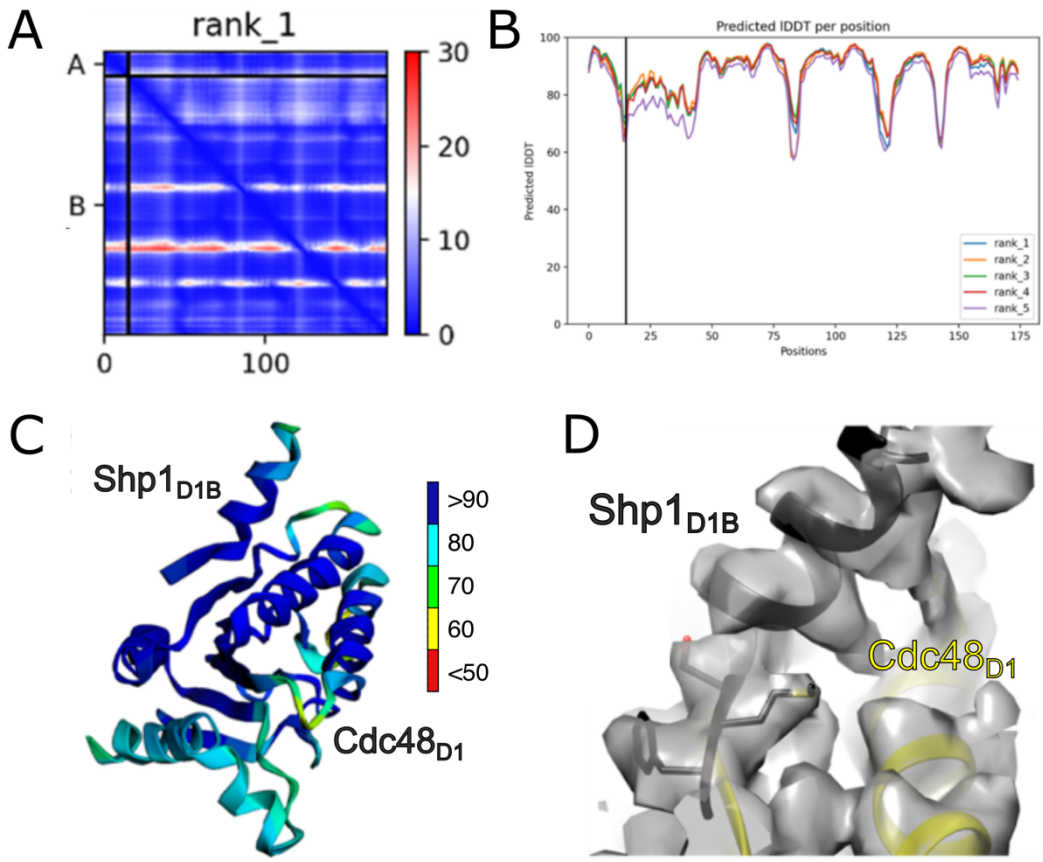

Supplementary Figure 15. ColabFold prediction of Shp1-Cdc48 interaction. (A) Predicted aligned error map for ColabFold prediction. Chain A, Shp1 D1B motif (residues 125-139); Chain B, Cdc48 D1 domain (residues 219-379). (B) Predicted local distance difference test (lDDT) scores for Shp1 D1B and Cdc48 D1. (C) Confidence scores for positions of predicted Shp1 D1B interactions with Cdc48 D1. (D) ColabFold predicted model of Shp1 D1B fitted as a rigid body into Cdc48 D1 of subunit C within the consensus reconstruction.

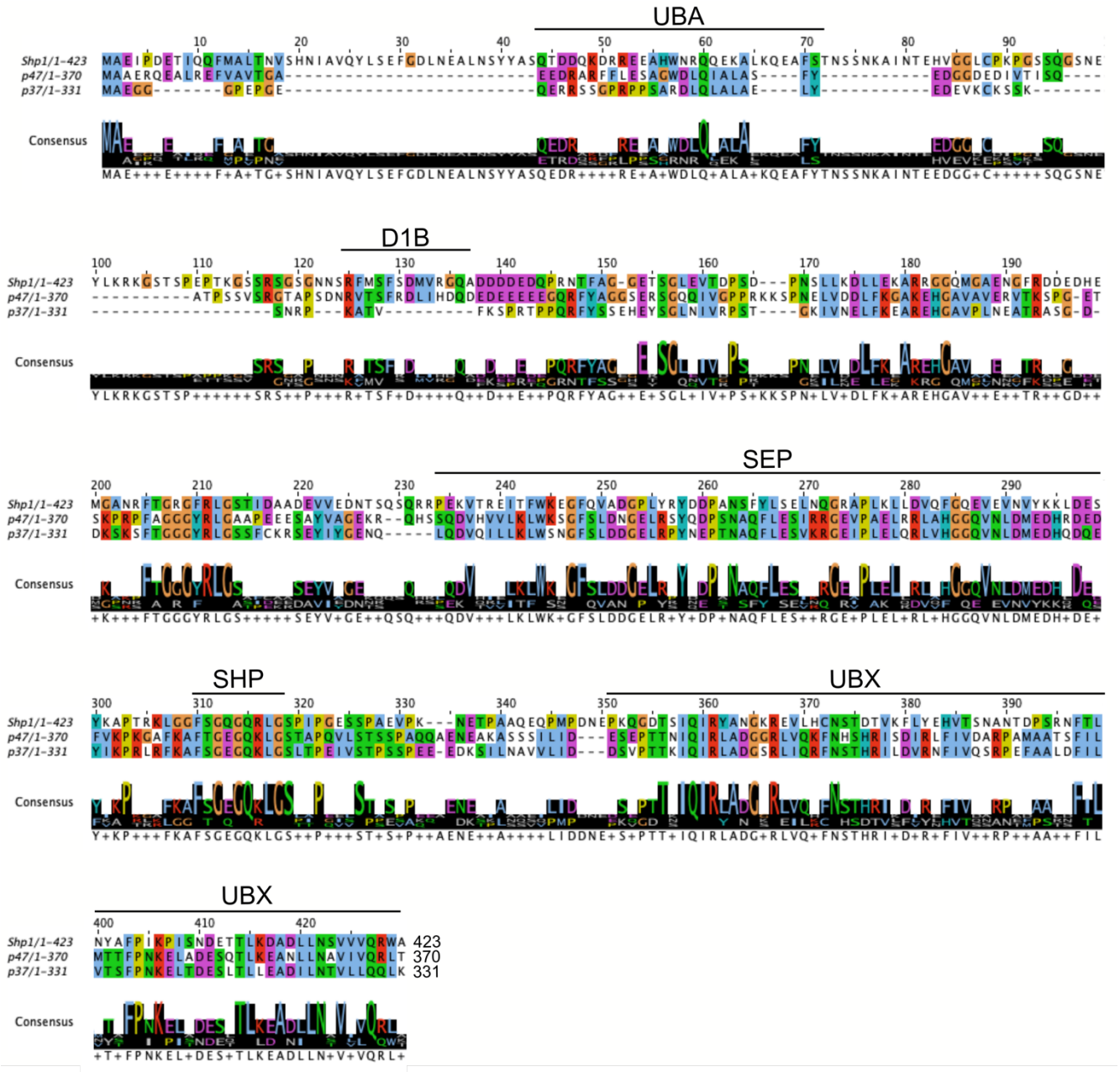

Supplementary Figure 16. Multiple sequence alignment among Shp1 (yeast) and its human orthologs, p47 and p37. Sequences queried: Shp1 (UniProt P34223), p47 (UniProt Q9UNZ2), and p37 (UniProt Q14CS0). Annotated domains indicated above sequences. Sequence alignment performed using Clustal Omega and figure created with Jalview.

Supplementary Table 1. Assigned nucleotide states for each subunit in classes 1-9 in D1 (left) and D2 (right).

D1

Class number	AB	BC	CD	DE	EF	FA
9	ATP	ATP	ATP	ADP	APO	APO
8	ATP	ATP	ATP	ADP	APO	APO
7	ATP	ATP	ATP	ADP	APO	APO
6	ATP	ATP	ATP	ADP/ATP	APO	APO
5	ATP	ATP	ATP	ATP	APO	APO
4	ATP	ATP	ATP	ATP	ADP/APO	APO
3	ATP	ATP	ATP	ATP	ADP	APO
2	ATP	ATP	ATP	ATP	ADP	APO
1	ATP	ATP	ATP	ATP	ADP	APO

D2

Class number	AB	BC	CD	DE	EF	FA
9	ATP	ATP	ATP	ADP	APO	ATP
8	ATP	ATP	ATP	ADP	APO	ATP
7	ATP	ATP	ATP	ADP/ATP	APO	ATP
6	ATP	ATP	ATP	ATP	ADP/APO	APO
5	ATP	ATP	ATP	ATP	ADP	APO
4	ATP	ATP	ATP	ATP	ADP	APO
3	ATP	ATP	ATP	ATP	ADP	APO
2	ATP	ATP	ATP	ATP	ADP	APO
1	ATP	ATP	ATP	ATP	ADP	APO

Supplementary Table 2. Validation Statistics (1/2)

	Consensus	**Class 1**	**Class 2**	**Class 3**	**Class 4**
EM Databank Accession ID	EMD-42076	EMD-41992	EMD-42038	EMD-42057	EMD-42045
Protein Data Bank Accession ID	8UB4	8U7T	8U9P	8UAA	8U8I
Collection and Data Processing					
Nominal Magnification	81,000x				
Defocus Range (μm)	0.5 - 2.5				
Number of micrographs	5,847				
Initial particle images	4,690,491				
Symmetry imposed	C1				
Final Particle images	325,377	41,227	45,203	42,875	22,656
Map Resolution FSC 0.143 (Å)					
Masked	2.9	3.3	3.2	3.4	3.5
Unmasked	3.6	6.4	6.2	6.5	7.7
Validation					
Starting model used (PDB code)	6OPC	6OPC	6OPC	6OPC	6OPC
Map Correlation coefficient	0.77	0.76	0.78	0.80	0.75
Atoms	23,006	22,832	23,283	23,381	21,316
Protein residues	3,274	3,209	3,255	3,211	3,177
Bonds (RMSD)					
Length (Å)	0.004 (0)	0.003 (0)	0.005 (0)	0.003 (0)	0.003 (0)
Angles (°)	0.591 (19)	0.642 (2)	0.748 (1)	0.666 (1)	0.665 (2)
MolProbity score	1.61	1.75	1.89	1.75	1.85
Clashscore	4.69	6.69	9.49	6.93	7.88
Ramachandran plot (%)					
Outliers	0	0.03	0.03	0.06	0.03
Allowed	5.40	5.49	5.80	5.25	6.31
Favored	94.53	94.48	94.17	94.68	93.66
Rotamer outliers (%)	0	0.15	0.24	0	0.44
Cß outliers (%)	0	0	0	0	0
CaBLAM outliers (%)	3.89	3.65	3.58	3.41	3.82

Supplementary Table 2. Validation Statistics, continued (2/2)

	Class 5	**Class 6**	**Class 7**	**Class 8**	**Class 9**
EM Databank Accession ID	EMD-42032	EMD-42039	EMD-42042	EMD-42043	EMD-42047
Protein Data Bank Accession ID	8U9C	8U9Q	8U9Z	8UA0	8UA1
Collection and Data Processing					
Nominal Magnification	81,000x				
Defocus Range (μm)	0.5 - 2.5				
Number of micrographs	5,847				
Initial particle images	4,690,491				
Symmetry imposed	C1				
Final Particle images	16,846	6,164	14,639	35,398	29,717
Map Resolution FSC 0.143 (Å)					
Masked	3.7	4.3	3.8	3.5	3.4
Unmasked	7.9	9.1	7.9	6.9	6.9
Validation					
Starting model used (PDB code)	6OPC	6OPC	6OPC	6OPC	6OPC
Map Correlation coefficient	0.77	0.76	0.77	0.78	0.80
Atoms	23,284	22,878	22,973	22,897	22,550
Protein residues	3,258	3,268	3,238	3,224	3,210
Length (Å)	0.003 (0)	0.003 (0)	0.003 (0)	0.003 (0)	0.004 (0)
Angles (°)	0.705 (5)	0.665 (2)	0.786 (6)	0.706 (6)	0.701 (1)
MolProbity score	1.78	1.81	1.95	1.80	1.71
Clashscore	7.79	8.07	11.58	6.93	6.69
Ramachandran plot (%)					
Outliers	0.03	0.03	0.06	0.03	0.03
Allowed	5.14	5.45	5.36	6.21	4.89
Favored	94.83	94.52	94.57	93.76	95.08
Rotamer outliers (%)	0.19	0	0.25	0.60	0.47
Cß outliers (%)	0	0.03	0	0	0
CaBLAM outliers (%)	3.54	3.80	3.47	3.65	3.14